An Alternative Chua's Circuit Implementation

K.S. Tang
Department of Electronic Engineering
City University of Hong Kong
Tat Chee Avenue, Kowloon, Hong Kong
eekstang@cityu.edu.hk

K.F. Man
Department of Electronic Engineering
City University of Hong Kong
Tat Chee Avenue, Kowloon, Hong Kong
kman@ieee.org

Abstract— **This paper proposed a novel nonlinear smooth function to implement the Chua's circuit. This new function provides a similar smoothness as to the cubic polynomial function, but a faster response and a simpler circuitry can be obtained. Some bifurcation phenomena and the chaotic attractors are observed experimently from the practical circuit.**

I. INTRODUCTION

Chua's circuit [1], [2] has been widely used as the experimental vehicle for chaotic and nonlinear research. Its schematic circuit is depicted in Fig. 1.

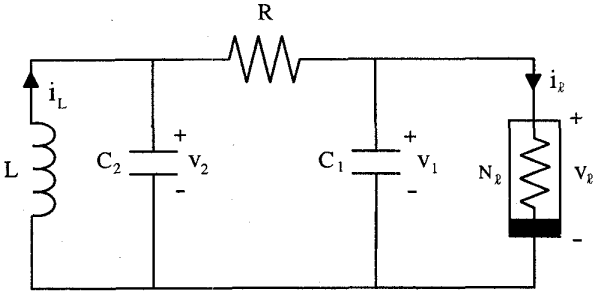

Fig. 1. Chua's circuit

The state equations of Chua's circuit can be expressed as

$$\begin{aligned}\frac{dv_1}{dt} &= \frac{1}{C_1}\left[\frac{1}{R}(v_2 - v_1) - g(v_1)\right] \\ \frac{dv_2}{dt} &= \frac{1}{C_2}\left[\frac{1}{R}(v_1 - v_2) + i_L\right] \\ \frac{di_L}{dt} &= \frac{1}{L}[v_2 - R_0 i_L] \end{aligned} \quad (1)$$

where R_0 denotes the small positive resistance of the inductor; $g(v_R)$ is a piecewise-linear function realized by Chua's diode (N_R) and defined as

$$\begin{aligned} g(v_R) &= i_R \\ &= G_b v_R + \frac{1}{2}(G_a - G_b)[|v_R + E| - |v_R - E|] \end{aligned} \quad (2)$$

with constant G_a, G_b and E.

This nonlinear v_R—i_R characteristics is an odd symmetric function with respect to origin. Due to its non-smoothness and non-differentiable at the turning points, cubic polynomial function has been proposed to substitute this piecewise-linear function [5]. In this paper, a novel nonlinear function is proposed. This new function provides a similar smoothness as to the cubic polynomial function, but a faster response and a simpler circuitry can be obtained.

II. CHAOTIC PHENOMENON IN PROPOSED FUNCTION

The proposed function is expressed as follows:

$$\bar{g}(v_R) = a \cdot v_R + b \cdot v_R|v_R| \quad (3)$$

where $a < 0$ and $b > 0$.

The equilibrium points can be calculated on the basis of the DC equilibrium circuit. Fig. 2 depicts the v_R—i_R characteristics of the proposed circuit and the load line. The equilibrium points are derived at 0 and ±1.5676.

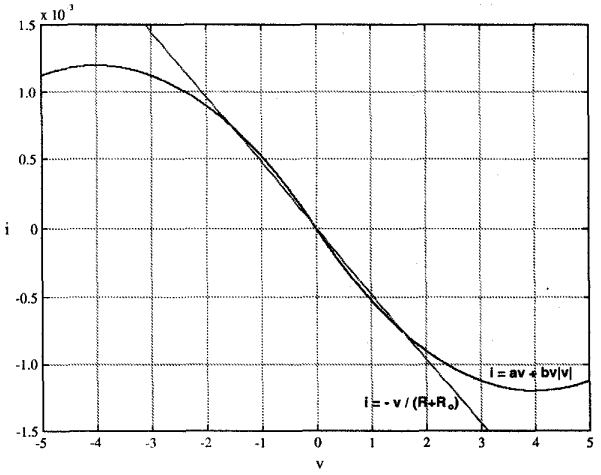

Fig. 2. v_R—i_R characteristic and d.c. load line with $R = 2060\Omega$, $R_0 = 14.99\Omega$, a=-0.5995mS and b=0.075mS/V

The eigenvalues at equilibrium points, 1.5676 or -1.5676, are 1.25548×10^5 and $-5082.94 \pm 25400.1j$, satisfying the Shil'nokov inequality, Appendix A [3].

The chaotic phenomenon can be observed via the bifurcation process, which is shown in Fig. 3 with respect to $\frac{1}{R}$. This bifurcation is considered to be compatible with those obtained in [4].

III. CIRCUITRY REALIZATION AND EXPERIMENTS

The electronic circuit for realizing (3) is shown in Fig. 4. It consists of two Op-amp (AD711 and LF347), one multiplier (AD633), one comparator (LM319) and an analog multiplexer (74HC4052). The LM319 and 74HC4052 provide a fast solution of the absolute function. LF347 works as a voltage follower. The Opamp AD711kN and the resistors R_2, R_3, R_4 form an equivalent negative resistance R for a ($a < 0$). When $R_2 = R_3$, $R = -R_4$. The Opamp AD711 is assumed to be operated in its linear region so that $a < 0$ and $b > 0$.

0-7803-4756-0/98/$10.00 1998 IEEE

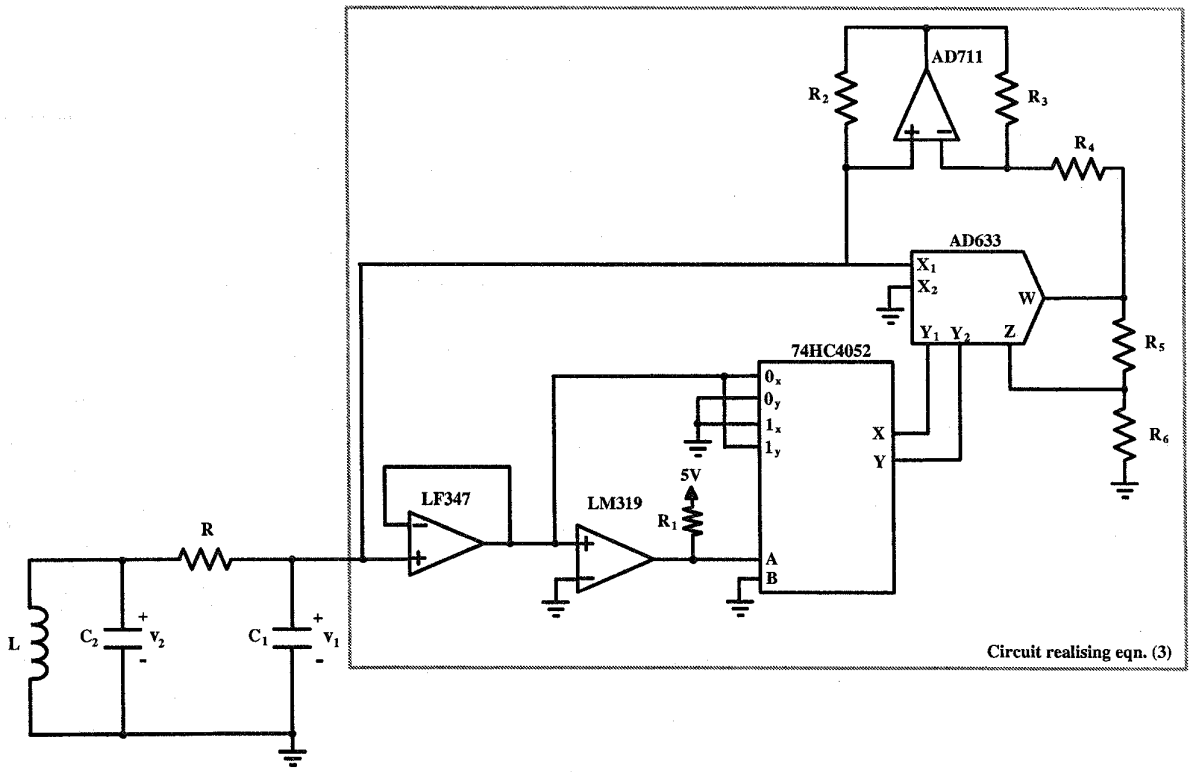

Fig. 4. Practical circuit diagram

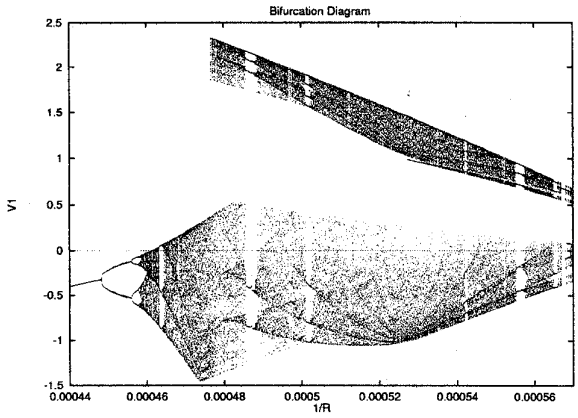

Fig. 3. Bifurcation diagram with $C_1 = 7nF$, $C_2 = 78nF$, $L = 18.84mH$, $R_0 = 14.99\Omega$, a=-0.5995mS and b=0.075mS/V

The driving-current for the $v_{\mathcal{R}}$—$i_{\mathcal{R}}$ characteristics of the proposed circuit is stated as below:

$$i_{\mathcal{R}} = \bar{g}(v_{\mathcal{R}}) = -\frac{1}{R_4} v_{\mathcal{R}} + \frac{R_5 + R_6}{R_4 R_5} \frac{1}{10V} v_{\mathcal{R}} |v_{\mathcal{R}}| \quad (4)$$

where the factor 10V is an inherent scaling voltage in the multiplier AD633.

Based on (3), we therefore have $a = -\frac{1}{R_4}$ and $b = \frac{R_5+R_6}{R_4 R_5} \frac{1}{10V}$. These coeffients, a and b, can be adjusted independently with different values of R_4, R_5 and R_6. The scale factor $\frac{R_5+R_6}{R_5}$ is limited to 100 for a practical application. In general, $R_5 \geq 1k\Omega$ and $R_6 \leq 100k\Omega$.

With the cubic approximation model proposed in [5], two multipliers are required. Whereas only one multiplier is required by this approach as indicated in Fig. 4. By the same token, the settling time delay is about half of the one in [5] which also implies that the response time at high frequency mode will be more exact. The typical settling time of different components used in both circuits is tabulated in Table I.

TABLE I
SETTLING TIME OF DIFFERENT COMPONENTS

Device	Settling time
AD633	2 μs
74HC4052	20ns
LM319	80ns

In our experiments, the resistor R is varied with the following components fixed:

$$R_1 = 1k\Omega,\ R_2 = R_3 = 2k\Omega,$$
$$R_4 = 1695\Omega,\ R_5 = 3k\Omega,\ R_6 = 750\Omega,$$
$$C_1 = 7nF,\ C_2 = 78nF$$
$$L = 18.84mH$$

Refer to (4), the computed values of a and b based on the above components are:

$$a = -0.590mS,\ b = 0.0737mS/V \quad (5)$$

Figs. 5–8 show the phase portraits in v_1—v_2 plane of different modes showing the existing of limit cycles, spiral Chua's attractor, double scroll Chua's attractor in such practical circuit.

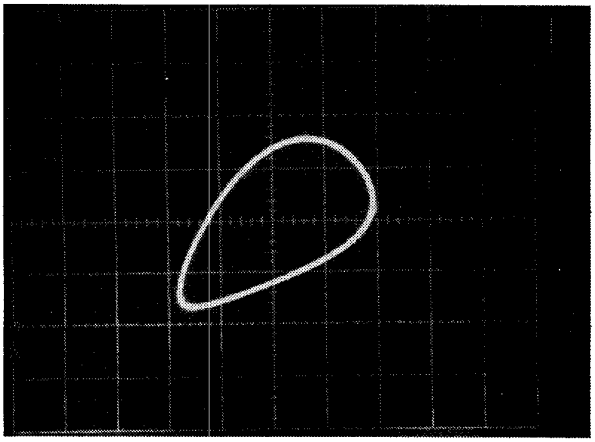

Fig. 5. Period 1 limit cycle: $R = 2350\Omega$, x-axis 1V/div and y-axis 0.5V/div

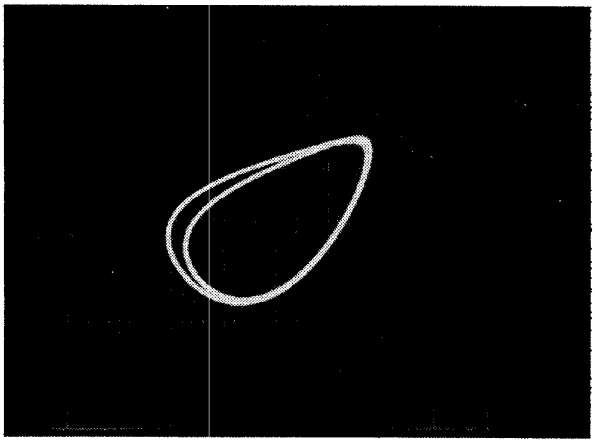

Fig. 6. Period 2 limit cycle: $R = 2340\Omega$, x-axis 1V/div and y-axis 0.5V/div

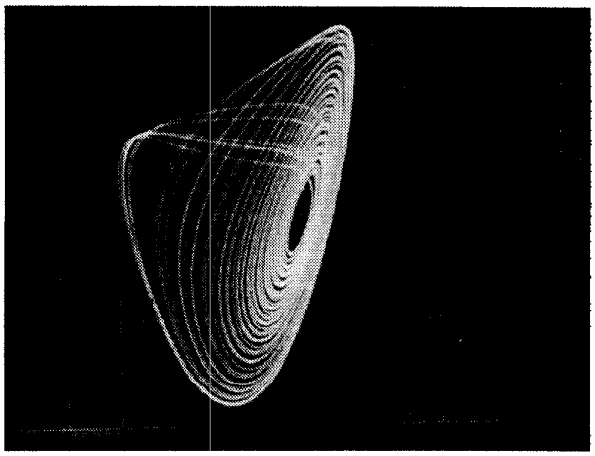

Fig. 7. Spiral: $R = 2260\Omega$, x-axis 1V/div and y-axis 0.2V/div

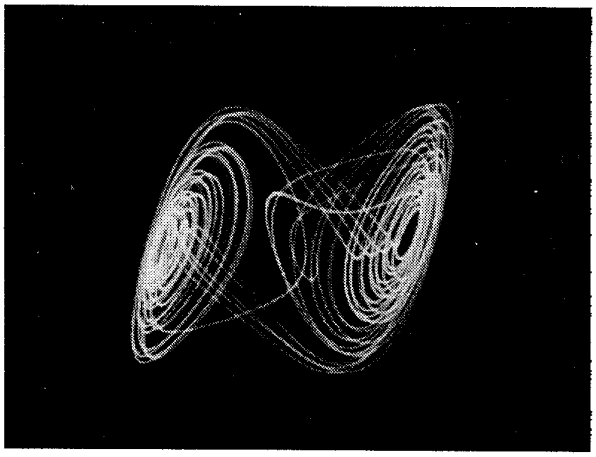

Fig. 8. Double scroll: $R = 2080\Omega$, x-axis 1V/div and y-axis 0.2V/div

IV. CONCLUSION

A novel nonlinear function with smooth nonlinearity is proposed in this paper for the study of Chua's circuit. It provides as an improved version of the cubic polynomial as far as circuitry simplicity, time response and cost. Both simulation runs and experimental results have clearly demonstrated the chaotic phenomenon obtained by the use of this nonlinear function.

V. REFERENCES

[1] *Special issue on chaos in nonlinear electronic circuits: Part A. Tutorials and reviews*, edited by L.O. Chua and M. Haster, *IEEE Trans. Circuit and Systems-I:Fundamental Theories and Applications*, vol. 40, no. 10, Oct 1993.

[2] L.P. Shil'nikov, "Chua's circuit: Rigorous results and future problems," *Int. J. Bifurcation and Chaos*, vol. 4, no. 3, 1994, pp. 489-519.

[3] C.P. Silva, "Shil'nikov's Theorem — A Tutorial," *IEEE Trans. Circuit and Systems-I:Fundamental Theories and Applications*, vol. 40, no. 10, Oct 1993, pp. 675–682.

[4] C.W.Wu and N.F.Rul'kov, "Studying Chaos via 1-D Maps - A Tutorial" *IEEE Trans. Circuit and Systems-I:Fundamental Theories and Applications*, vol. 40, no. 10, Oct 1993, pp. 707–721.

[5] G.Q. Zhong, "Implementation of Chua's circuit with a cubic nonlinearity," *IEEE Trans. Circuit and Systems-I:Fundamental Theories and Applications*, vol. 41, no. 12, Dec 1994, pp. 934–941.

APPENDIX A: SHIL'NOKOV THEOREM

Consider the third-order dynamical system

$$\frac{d\mathbf{x}}{dt} = \xi(\mathbf{x}), \quad t \in \Re, \quad \mathbf{x} \in \Re^3 \tag{A.1}$$

where the vector field $\xi : \Re^3 \rightarrow \Re^3$ is p-times differentiable ($p \geq 1$) with a continuous derivative (called class C^p).

The equilibrium point $\mathbf{x}_e$ for (A.1) is a *hyperbolic saddle focus* (or saddle focus) if the eigenvalues of the 3×3 Jacobian derivative of ξ at $\mathbf{x}_e$, are of the form

$$\gamma, \sigma \pm j\omega, \quad \sigma\gamma < 0, \quad \omega \neq 0 \tag{A.2}$$

where γ, σ, and ω are real.

There are some basic terminology related with the special orbits that lie at the heart of the Shil'nikov approach.

- *Homoclinic orbit* $\mathcal{H}$ based at a hyperbolic saddle focus $\mathbf{x}_e$ is a bounded dynamical trajectory that is doubly asymptotic to the equilibrium point.
- *Heteroclinic orbit* is similar to homoclinic orbit except that there are two distinct saddle foci being connected, one corresponding to the forward asymptotic time limit and the other to the reverse asymptotic time limit.
- *Heteroclinic loop* is formed by the union of two or more heteroclinic orbits.

Given the third-order autonomous system in (A.1), where ξ is a C^2 vector field on $\Re^3$, and let $\mathbf{x}_{e1}$ and $\mathbf{x}_{e2}$ be two distinct equilibrium points for (A.1),
if

1. Both $\mathbf{x}_{e1}$ and $\mathbf{x}_{e2}$ are saddle foci that satisfy the Shil'nikov inequality

$$|\gamma_i| > |\sigma_i| > 0, \quad (i = 1, 2) \tag{A.3}$$

with the further constraint

$$\sigma_1 \sigma_2 > 0 \quad \text{or} \quad \gamma_1 \gamma_2 > 0 \tag{A.4}$$

2. There is a heteroclinic loop $\mathcal{H}_L$ joining $\mathbf{x}_{e1}$ to $\mathbf{x}_{e2}$ that is made up of two heteroclinic orbits $\mathcal{H}_i$ $(i = 1, 2)$

then

1. The Shil'nikov map defined in a neighborhood of $\mathcal{H}_L$ possesses a countable number of Smale horseshoes in its discrete dynamics;
2. For any sufficiently small C^1-perturbation ζ of ξ^2, the perturbed system

$$\frac{d\mathbf{x}}{dt} = \zeta(\mathbf{x}), \quad t \in \Re, \quad \mathbf{x} \in \Re^3 \tag{A.5}$$

has at least a finite number of Smale horseshoes in the discrete dynamics of the Shil'nikov map defined near $\mathcal{H}_L$

3. Both the original (A.1) and the perturbed one (A.5) exhibit horseshoe chaos (also known as heteroclinic chaos)